IEICE Proceeding Series

Analysis of Intermittent Time Series: How to Discriminate the Different States of an Interior Crisis

Thomas Stemler, Thomas Jüngling

Vol. 1 pp. 377-380
Publication Date: 2014/03/17
Online ISSN: 2188-5079

2012 International Symposium on Nonlinear Theory and its Applications
NOLTA2012, Palma, Majorca, Spain, October 22-26, 2012

Analysis of Intermittent Time Series: How to Discriminate the Different States of an Interior Crisis

Thomas Stemler† and Thomas Jüngling‡

†School of Mathematics and Statistics, The University of Western Australia
35 Stirling Highway Crawley, Perth, 6009 Australia
‡Lehrstuhl für Theoretische Physik III, Institut fr Theoretische Physik und Astrophysik, Universität Würzburg
Am Hubland, 97074 Würzburg, Germany
Email: thomas.stemler@uwa.edu.au, thomas.juengling@physik.uni-wuerzburg.de

Abstract—Intermittency is the textbook example of a dynamics having different time scales: A fast dynamics in the state and a slow jumping dynamics between them. Sometimes it is quite easy to distinguish the different kind of dynamics, since the states are well separated. An example of this kind of dynamics is the intermittent dynamics generated by a merging crisis: the states and sub–attractors are mirror images of each other and therefore can be distinguished without effort. Here we report on a different kind of crisis–induced intermittency, resulting from an interior crisis. Especially if only one state variable of the system can be observed, it is difficult to determine the state in which the system currently is. We show that our method is able to identify the states accurate using numerical data from the logistic map and measurements from a diode oscillator.

1. Introduction

In nature systems often show dynamics on different time scales. For example fast turbulent dynamics is a main feature of our earth's atmosphere which is coupled to the much slower oceans. It is obvious from this example that one cannot and moreover might not want to model such a complex system in all details. But before we can use stochastic modelling or other methods to reduce the dimensionality of a model, we need to understand how fast chaotic degrees of freedom impact on the slow dynamics.

One class of systems that allows us to study this interplay of fast and slow degrees of freedom are systems showing crisis–induced intermittency. In these systems a fast chaotic motion in the states lead to a slow switching dynamics between the states. Ott, Grebogi and York explored the statistics of the switching dynamics and found universal scaling laws for the different kind of intermittency scenarios[1]. Since then intermittent systems have been intensively studied, using numerical low–dimensional models[2] as well as experimental data from high–dimensional systems[3]. They are a good arch–systems to test stochastic modelling[4] and just like stochastic systems they show stochastic resonance[5, 6, 7, 8].

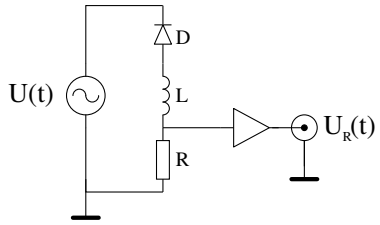

Figure 1: Diode resonator circuit consisting of a $1N4006$ diode, an inductor $L = 1\text{mH}$, a resistor $R = 51\Omega$, and a sinusoidal drive $U(t) = U_0 \sin(\Omega t)$ with amplitude $U_0 = 0\text{V} \ldots 6\text{V}$ and frequency $\Omega/2\pi = 1\text{MHz}$. Additional components for shielding and extracting the signal which were implemented to minimise noise and cross-talk are not shown.

Here we present an investigation that just wanted to verify that in another class of crisis stochastic resonance occurs as well. Like often it turned out that the road we had to travel, to get this verification, was much more interesting than the result itself. We focussed on an experimental system that shows intermittency due to an interior crisis. Unlike merging crisis that have certain symmetries it is much harder to distinguish between the different states. After we introduced the experimental system in the next section, we explain how we were able to distinguish the different states in the time series analysis by using a return map. Given the page restriction we are unable to explain the observed stochastic resonance. But one can find the results in ref.[9].

2. Experimental Setup

Experimental data is somehow superior to just numerical data. When conducting experiments the usual "real world" effects, like parameter drifts, dynamical and measurement noise, influence the outcomes. In addition the length of the time series is often restricted. Therefore a verification based on experimental data somehow guaranties robustness.

We analysed data from a diode resonator, shown in Fig.1. It is one of the simplest electronic circuits showing chaotic dynamics. The non–autonomous circuit is driven by a si-

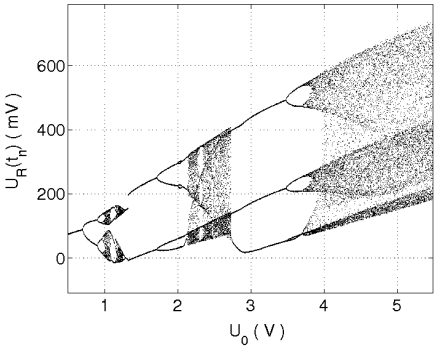

Figure 2: Bifurcation diagram of the diode resonator constructed from the maxima of the output signal $U_R(t)$ at discrete times t_n.

nusoidal signal using an Agilent 33220A signal generator. Note that we chose the amplitude of this signal U_0 as our control parameter and kept the frequency constant at 1 MHz. We recorded the output signal $U_R(t)$ using a Signatec DA500A transient card with a maximum sampling rate of 500MS/s.

To gain an understanding of the dynamics we record the time series of U_R as a function of U_0 and generated the bifurcation diagram shown in Fig.2. As we can see the oscillator follows a period–doubling route to chaos. We are especially interested in the region around the period–three window: $U_0 = 2.7\text{V} \ldots 4.0\text{V}$. At $U_0 = 2.7\text{V}$ the window opens in a saddle node bifurcation where a pair of stable and unstable period-three orbits is generated. As we can see for control parameters above $U_0 = 3.5\text{V}$ the period–three undergoes several period–doubling bifurcation and around $U_0 \approx 3.8\text{V}$ a chaotic attractor is formed. This chaotic attractor collides with an unstable periodic orbit at $U_c = U_0 = 4\text{V}$ which is the critical control parameter for the crisis. This collision causes an interior crisis, which is clearly visible in the bifurcation diagram by an abrupt widening of the chaotic attractor. For our later analysis we name the chaotic dynamics on the first attractor between $U_0 = [3.8, ..., 4.0]\text{V}$ "Ch1" and the new part of the phase space occurring after the crisis "Ch2". For control parameters above U_c the dynamics of the oscillator is characterised by a fast dynamics in Ch1 or Ch2 and switching between these states. In Fig.3 we see an example of the dynamics before and after the crisis. This figure also explains the principle problem we have when analysing such data sets: the two states are convoluted in such a way that a simple threshold method will not be able to distinguish between the states. In systems showing intermittency due to a merging crisis such a method only works because of the symmetry of the states[8]. In interior crisis the states are quite asymmetrical and one need to apply more advanced methods.

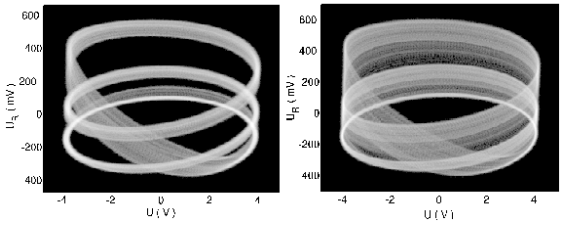

Figure 3: Density plots showing the projection of the attractor onto the U-U_R-plane as a screen shot from an analog oscilloscope. Left: Driving amplitude $U_0 < U_c = 4.0V$. Right: $U_0 > U_c$.

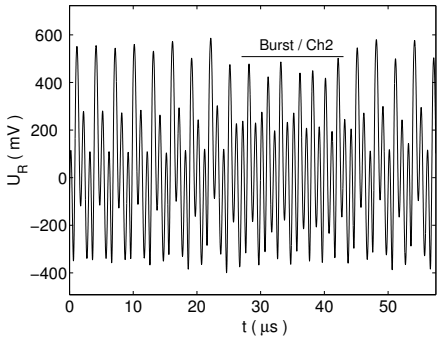

Figure 4: Typical time trace in the intermittent regime showing a single burst.

3. Identifying the different states

Fig.4 shows a typical time series we want to analyse. The highlighted part of the time series is one of the regions where we have a short burst into the Ch2 state. As we can see such a region is characterised by U_R no longer showing the period–three motion in the Ch1 state. Obviously this periodicity results from the former stable period–three orbit. While one might want to try averaging techniques, previously successful applied to intermittent time series[3], the chaotic motion in Ch1 will make such a method unreliable especially for $U_c \geq 4.5\text{V}$. We therefore derived a criterion bases on a return map.

For simplicity we are going to introduce this method by analysing the interior crisis of the logistic map:

$$x_{n+1} = rx_n(1 - x_n) \equiv M_r(x_n) \; . \tag{1}$$

As we can see in Fig.5 the logistic map has a similar interior crisis. But unlike in the diode resonator we can analytical determine the boundaries between the two states as well as the unstable period-three orbit. At $r_c \approx 3.8568$ the crisis occurs. Afterwards the first six images of $g_0 = x = 1/2$, $g_n(r) = M_r^n(1/2)$, $n = 1, 2 \ldots, 6$ determine the boundary of the Ch1 state for $r - r_c \approx 0$, since the critical point is contained in one of the chaotic bands and the three intervals are mapped onto each other [2]. Beyond the crisis, for $r > r_c$, the borderline functions $g_n(r)$ are smooth continuations of the precritical attractor defining the Ch1 state. For

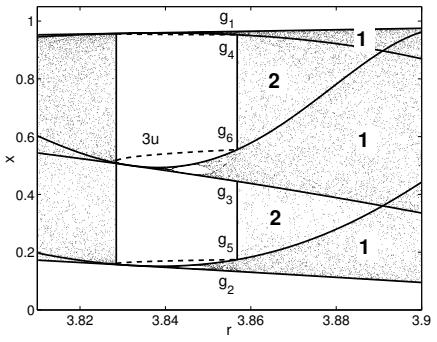

Figure 5: Skeleton of the logistic map in a neighbourhood of the period three window. Solid lines: first six iterates $g_n(r)$ of the critical point; broken line: unstable period-three orbit. Labels refer to the phases 'Ch1' and 'Ch2'.

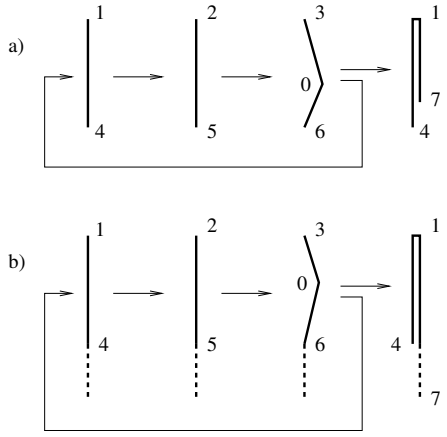

Figure 6: Diagrammatic view of the folding and stretching process of a chaotic three-band attractor. a) Below the crises. Labels refer to the images of the 'critical point' g_0, solid lines visualise the three bands which are mapped onto each other. b) Beyond the crises. Dashed lines indicate those parts which are not mapped onto each other any more.

maps with critical points these boundaries can be observed as significant structures in the invariant density. They arise from folding the phase space during one iteration step. Since the derivative vanishes at the critical point a high density is created at the next image points g_n. For higher iterations the density decays due to the stretching mechanism of chaotic maps. This general mechanism constitutes the basis of our further analysis. Symbolic dynamics tells us that the three intervals $[g_2, g_5]$, $[g_3, g_6]$, and $[g_4, g_1]$ constitute the period-three chaotic state for $r < r_c$ while the gaps are determined by (g_5, g_3) and (g_6, g_3). Thus, even beyond the crisis we can define the two different chaotic phases, Ch1 and Ch2, by the symbolic variable

$$\sigma_n = \begin{cases} +1 & \text{if } x_n \in (g_5, g_3) \cup (g_6, g_4) \\ -1 & \text{if } x_n \in [g_2, g_5] \cup [g_3, g_6] \cup [g_4, g_1] \end{cases} \qquad (2)$$

We now turn to the identification of the different dynamical regimes in our experimental system. An appropriate return map $u_n \mapsto u_{n+1}$ can be constructed from the local maxima $u_n \equiv U_R(t_n)$ of the time series. By projecting the three–dimensional chaotic system onto a single dimension (see. Fig.7), we get a structure that is far more complex than the one of the logistic map. In contrast to the logistic map the projection of the three branches of the experimental band attractor are no longer separated but partly overlap. Even more, the Ch1 and Ch2 phases are highly intermingled and we need a more sophisticated tool than eq. (2) to separate the states.

Despite these difficulties the main ideas developed in the context of the logistic map can be used. Again, the maximal value of the amplitude

$$g_1 = \max_n\{u_n\} = \max_t\{U_R(t)\} \ . \qquad (3)$$

is of crucial importance. If our dynamical system were the logistic map then one of the preimages would be the critical point g_0 causing the folding of the phase space. Similar topological considerations apply to our experimental results as well (cf. fig.7). The following five recursive images $g_2, \ldots, g_6$, are again boundary points for each of the three branches. Below the crisis, for $U_0 < U_c$, one can clearly observe that the different branches of the Ch1 attractor are mapped onto each other and just like in the logistic map visited in a well-defined sequence (cf. Fig.6a). After the crisis the combined folding and stretching maps some of the images outside the starting branch (cf. fig.6b), generating the Ch2–phase. The return map is neither a single valued function nor are the different branches of the phases well separated when projected onto the horizontal axis. Therefore we cannot apply a threshold condition on the amplitudes u_n, like eq.(2). But if we take into account how the different branches of our return map are mapped onto each other we can develop a simple recipe to decompose the time series. The points g_1 and g_4 can be used to isolate the non-overlapping first branch of the Ch1 phase. If $u_n \in [g_4, g_1]$ we assign the symbol $\sigma_n = -1$ to this event and to the two following iterates. Those data points which after three iterations do no longer fit into the branch cycle fig.6 are attributed to the phase Ch2 by assigning a symbolic coordinate with positive value. The symbol remains $\sigma_n = -1$ until another event $u_n \in [g_4, g_1]$ is detected. By exploiting this technique the experimental time series can be converted into a symbolic sequence, as was already demonstrated for the logistic map. We use this sequence for further analysis, e.g. for the evaluation of the mean residence times $\langle\tau_1\rangle$ and $\langle\tau_2\rangle$ of the two different phases, 'Ch1' and 'Ch2', respectively. The dependence of the mean residence time on the control parameter U_0 is shown in fig.8. The mean 'laminar' residence time $\langle\tau_1\rangle$ follows a power law [1, 2, 10, 11]. The exponent is related to the geometric properties of the attractor. The mean 'burst' residence time $\langle\tau_2\rangle$ tends to a finite limit when approaching the crisis. An-

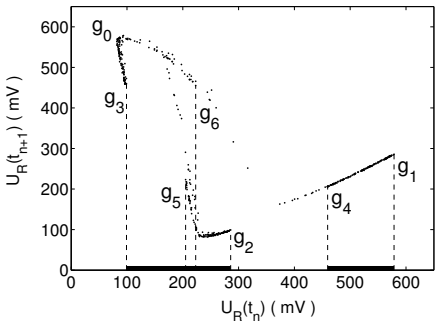

Figure 7: Return map constructed from the local maxima of the experimental time series $U_R(t)$ close to the crisis. Labels refer to the critical point and its images. The rightmost branch of the 'Ch1'-phase remains well separated, while the other branches overlap with each other and with parts of the 'Ch2'-phase.

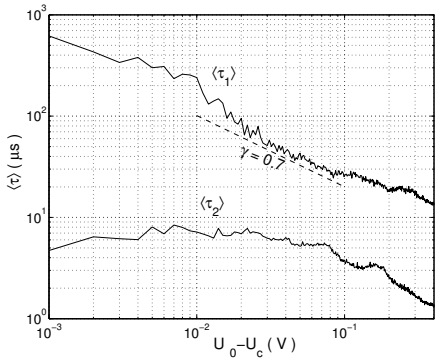

Figure 8: Mean residence times of the diode resonator evaluated from the symbolic time series. $\langle \tau_1 \rangle$ follows a power law with a scaling exponent γ of 0.7 as predicted in [1].

alytic expressions for scaling exponents have been derived in [12] for one-dimensional maps.

4. Conclusion

We started this investigation since a major constraint for the identification of our stochastic resonance phenomenon was caused by the proper identification of the different dynamical phases of the intermittent regime. As we have mentioned before details of the stochastic resonance can be found in Ref.[9].

We have ssen that for interior crisis the phases are highly intermingled and one cannot apply a simple threshold condition. We have employed here return maps and ideas borrowed from symbolic dynamics for the purpose of state identification. In such a way a quantitative criterion has been developed to separate the different dynamical phases which are related with the precritical attractor and the precritical chaotic repeller, respectively. The approach converts the time series into a symbolic representation which allows the accurate determination of mean residence times and for stochastic resonance cross correlation functions.

Acknowledgements

The authors would like to thank Kevin Judd (UWA) for useful comments and discussion.

References

[1] C. Grebogi, E. Ott, F. Romeiras, and J.A. Yorke. *Phys. Rev. A*, 36:5365, 1987.

[2] C. Grebogi, E. Ott, and J.A. Yorke. *Phys. Rev. Lett.*, 57:1284, 1986.

[3] J. Becker, F. Röedlsperger, Th. Weyrauch, H. Benner, W. Just, A. Cenys *Phys. Rev. E* 59:1622, 1999.

[4] T. Stemler, J.P. Werner, H. Benner, and W. Just. *Phys. Rev. Lett.*, 98:044102, 2007.

[5] L. Gammaitoni, P. Hänggi, P. Jung, and F. Marchsoni. *Rev. Mod. Phys.*, 70:223, 1998.

[6] E. Reibold, W. Just, J. Becker, and H. Benner. *Phys. Rev. Lett.*, 78:3101, 1997.

[7] A. Krawiecki, S. Matyjaskiewicz, K. Kacperski, and J.A. Hołyst. *Phys. Rev. E*, 64:041104, 2001.

[8] J. P. Werner, T. Stemler, H. Benner. *Physica D*, 237:859, 2008.

[9] T. Juengling, H. Benner, T. Stemler, W. Just. *Phys. Rev. E*, 77:036216, 2008.

[10] W.L. Ditto, S. Rauseo, R. Cawley, C. Grebogi, G.-H. Hsu, E. Kostelich, E. Ott, H.T. Savage, R. Segnan, M.L. Spano, and J.A. Yorke. *Phys. Rev. Lett.*, 63:923, 1989.

[11] K. Kacperski and J.A. Hołyst. *Phys. Lett. A*, 254:53, 1999. *Phys. Rev. E*, 60:403, 1999.

[12] C. Grebogi, E. Ott, and J.A. Yorke. *Phys. Rev. Lett.*, 48:1507, 1982.